



ELSEVIER

Contents lists available at ScienceDirect

Nuclear Instruments and Methods in Physics Research A

journal homepage: www.elsevier.com/locate/nima

Optimization of crystals for applications in dual-readout calorimetry

N. Akchurin^a, F. Bedeschi^b, A. Cardini^c, R. Carosi^b, G. Ciapetti^d, M. Fasoli^e, R. Ferrari^f, S. Franchino^g, M. Fraternali^g, G. Gaudio^f, J. Hauptman^h, M. Incagli^b, F. Lacava^d, L. La Rotondaⁱ, S. Lee^h, M. Livan^g, E. Meoni^{i,1}, M. Nikl^j, D. Pinci^d, A. Policicchio^{i,2}, S. Popescu^a, F. Scuri^b, A. Sill^a, G. Susinnoⁱ, W. Vandelli^k, A. Vedda^e, T. Venturelliⁱ, C. Voena^d, I. Volobouev^a, R. Wigmans^{a,*}

^a Texas Tech University, Lubbock (TX), USA^b Dipartimento di Fisica, Università di Pisa and INFN Sezione di Pisa, Italy^c INFN Sezione di Cagliari, Monserrato (CA), Italy^d Dipartimento di Fisica, Università di Roma "La Sapienza" and INFN Sezione di Roma, Italy^e INFN and Department of Materials Science, Università di Milano-Bicocca, Italy^f INFN Sezione di Pavia, Italy^g INFN Sezione di Pavia and Dipartimento di Fisica Nucleare e Teorica, Università di Pavia, Italy^h Iowa State University, Ames (IA), USAⁱ INFN Cosenza and Dipartimento di Fisica, Università della Calabria, Italy^j Institute of Physics, Prague, Czech Republic^k CERN, Genève, Switzerland

ARTICLE INFO

Article history:

Received 30 April 2010

Accepted 10 May 2010

Available online 9 June 2010

Keywords:

Calorimetry

Cherenkov light

High-Z scintillating crystals

ABSTRACT

We present a systematic study of lead tungstate crystals doped with a small fraction of molybdenum, varying between 0.1% and 5%. These crystals were exposed to a beam of 50 GeV electrons and the signals were unraveled into scintillation and Cherenkov contributions, using the time structure of the signals and/or different types of transmission filters. These studies were carried out in view of the possible application of such crystals in dual-readout calorimeters.

© 2010 Elsevier B.V. All rights reserved.

1. Introduction

High-density scintillating crystals have traditionally been the detectors of choice in particle physics experiments that required high-resolution measurements of electrons and photons produced in the interactions. However, experiments in which such crystals serve as the electromagnetic (em) section of the calorimeter system usually have poor performance when it comes to the detection of hadrons and jets [1]. This is a direct result of their very large e/h ratio, e.g., 2.4 for high-Z crystals such as lead tungstate (PbWO₄).

Recently, interest in using such crystals for the electromagnetic section of a general-purpose calorimeter system has been renewed because of the possibility to separate their signals into components deriving from Cherenkov light and scintillation light. This would open the way to use such crystals as *dual-readout calorimeters*. Event-by-event measurements of the em fraction of

showers induced by hadrons or jets, which is possible in such calorimeters, would eliminate the main reason for the poor hadronic performance.

In earlier papers, we have demonstrated that a significant fraction of the signal from scintillating PbWO₄ crystals is in fact due to Cherenkov radiation. At room temperature, Cherenkov light was found to contribute up to 15% of the signal generated by high-energy particles traversing a PbWO₄ crystal [2], and this fraction increased further with the temperature [3].

Studies with a BGO crystal [4] showed that it was possible to separate the two types of light effectively by means of filters, despite the fact that Cherenkov radiation represents only a small fraction of 1% of the light produced by this bright scintillator. Large differences between the spectral properties and the time structure of the two components made this possible.

Inspired by these successes, we decided to explore the possibility of combining these advantages of BGO with the intrinsically much higher Cherenkov fraction of PbWO₄ light. To this end, we developed a number of dedicated PbWO₄ crystals doped with small fractions of impurities chosen such as to achieve a shift of the scintillation spectrum to longer wavelengths, and a longer decay time. The first studies of these crystals showed that especially molybdenum doping gave promising results. It turned out to be possible to extract from

* Corresponding author. Tel.: +1 806 742 3779; fax: +1 806 742 1182.

E-mail address: wigmans@ttu.edu (R. Wigmans).¹ Current address: Department of Physics, University of Barcelona, Spain.² Current address: Department of Physics, University of Washington, Seattle (WA), USA.

these crystals almost pure Cherenkov or pure scintillation signals, simply by using adequate optical filters [5]. However, these studies also revealed some drawbacks, which made these crystals unsuitable for the intended use:

- (1) The Cherenkov signals were too small, < 10 photoelectrons per GeV.
- (2) The Cherenkov light was strongly attenuated, more than a factor of three over a distance of only 10 cm.

Based on our understanding of the reasons for these problems, we decided to develop a number of PbWO_4 crystals containing smaller fractions of molybdenum. This paper describes the test results of this new batch.

In Section 2, these crystals and the experimental setup in which they were tested are described, as well as the calibration and data analysis methods that were used. Experimental results are presented in Section 3. In the concluding Section 4, we discuss the implications of these results.

2. Equipment and measurements

2.1. Detectors and beam line

The measurements described in this paper were performed in the H4 beam line of the Super Proton Synchrotron at CERN. Our detector was a high-density lead tungstate crystal, doped with a small fraction of molybdenum. The molybdenum impurity substitutes the tungsten ion in the matrix and forms a MoO_4 complex, which has a large cross-section for electron capture, and acts as a wavelength shifter. Radioluminescence measurements carried out on samples of the crystals used in our studies indicated that the maximum of the emission shifted from ~ 420 to ~ 480 nm as a result of this doping, and that details of the emission spectrum depended somewhat on the precise amount of Mo, at least for the range used in this study (0.1–5%).

Lead tungstate crystals with Mo doping levels of 0.1%, 0.2%, 0.3%, 1% and 5% were produced by the Radiation Instruments & New Components company in Minsk (Belarus). We reported earlier on the 1% and 5% crystals, which were produced in 2008 [5]. The crystals with the smaller doping concentration were produced in 2009. All crystals had a length of 20 cm and a cross-section of $2.0 \times 2.0 \text{ cm}^2$. The transverse dimension, relevant for our measurements, corresponded to 2.25 radiation lengths (X_0). The light produced by particles traversing this crystal was read out by two photomultiplier tubes (PMTs) located at opposite ends. Hamamatsu R8900U tubes, with 10 multiplication stages and equipped with a borosilicate window and a Super Bi-Alkali photocathode, were used for this purpose.

We used different types of optical transmission filters to study the crystal signals. These filters were 3 mm thick, made of glass.³ Three different filters, known as UG11, U330 and UG5, were intended to increase the relative fraction of Cherenkov light, since they only transmitted light with short wavelengths. A yellow filter (known as GG495), which transmitted only light with wavelengths longer than the 495 nm cutoff value, was used to generate essentially pure scintillation signals.

In order to reduce the light trapping effects of the large refractive index of PbWO_4 ($n = 2.2$), the PMTs were coupled to the crystal by means of silicone “cookies” ($n = 1.403$). These cookies provided optical contact between the crystal end face and

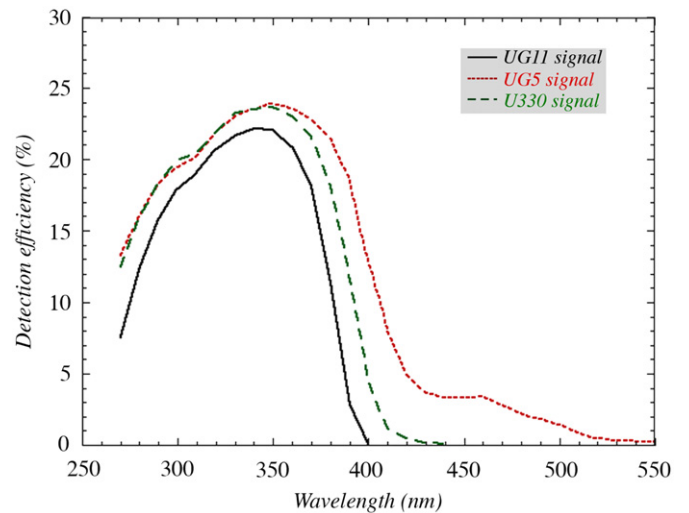


Fig. 1. Detection efficiency of light exiting the PbWO_4 crystal, as a function of the wavelength. Results are given for three different filters and include the effects of optical transmission through the filter and the silicone cookies, as well as the quantum efficiency of the photocathode. Data based on manufacturer's specifications.

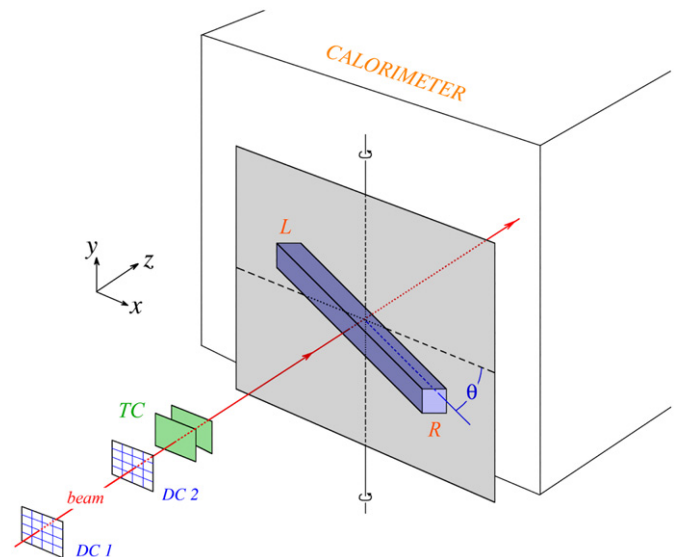


Fig. 2. Experimental setup in which the beam tests of the crystals were performed. The angle θ is negative when the crystal is oriented as drawn here. This drawing is schematic and *not* to scale.

the filter and between the filter and the PMT window. Fig. 1 shows the efficiency with which light exiting the crystal end face was detected in the PMT. Results are given as a function of wavelength and include the losses due to optical transmission through the filter and the silicone cookies, as well as the quantum efficiency of the PMT's photocathode. In the following, we quantify the differences between the three filters in a simplified way by means of an “effective cutoff wavelength”, set at 390, 400 and 410 nm for UG11, U330 and UG5, respectively.

The crystal under study was mounted on a platform that could rotate around a vertical axis. The crystal was oriented in the horizontal plane and the rotation axis went through its geometrical center. The particle beam was also steered through this center, as illustrated in Fig. 2. The angle θ , which is frequently used in the following, represents the angle between the crystal axis and a plane perpendicular to the beam line. The angle increased when the crystal was rotated such that the crystal axis

³ The UG11, UG5 and GG495 filters were produced by Schott, the U330 filter by Hoya.

L-R approached the direction of the traveling beam particles. The crystal orientation shown in Fig. 2 corresponds to $\theta = -30^\circ$.

Two small scintillation counters (TC) provided the signals that were used to trigger the data acquisition system. These trigger counters were 2.5 mm thick, and the area of overlap was $6 \times 6 \text{ cm}^2$. A coincidence between the logic signals from these counters provided the trigger. The trajectories of individual beam particles could be reconstructed with the information provided by two small drift chambers (DC1, DC2) which were installed upstream of the trigger counters. This system made it possible to determine the location of the impact point of the beam particles at the calorimeter with a precision of typically $\sim 0.2 \text{ mm}$. About 10 m downstream of the crystal, placed behind about 20 interaction lengths of material, a $50 \times 50 \text{ cm}^2$ scintillator paddle served as a muon counter. The first 10 interaction lengths consisted of the DREAM fiber calorimeter [6,7], which in this study only served to recognize and eliminate hadrons contaminating the electron beam.

2.2. Data acquisition

Measurement of the time structure of the crystal signals formed a very important part of the tests described here. In order to limit distortion of this structure as much as possible, we used special 15 mm thick low-loss cables to transport the crystal signals to the counting room. Such cables were also used for the signals from the trigger counters, and these were routed such as to minimize delays in the DAQ system.⁴ Other signals, e.g., from the muon counter and the calorimeter, were transported through RG-58 cables with (for timing purposes) appropriate lengths to the counting room.

The data acquisition system used VME electronics. A single VME crate hosted all the needed readout and control boards. The signals from the calorimeter channels and the muon counter were integrated and digitized with a sensitivity of 100 fC/count, on 12-bit QDC V792 CAEN modules. The timing information of the tracking chambers was recorded with 1 ns resolution in a 16-bit 16-channel LeCroy 1176 TDC.

The time structure of the calorimeter signals was recorded by means of a Tektronix TDS 7254B digital oscilloscope,⁵ which provided a sampling capability of 5 GSamples/s, at an analog bandwidth of 2.5 GHz, over four input channels. For the tests described in this paper, only two channels were sampled. The oscilloscope gain (scale) was tuned such as to optimize the exploitation of the 8-bit dynamic range, i.e., by choosing the sensitivity such that the overflow rate was $< 1\%$.

The crystal signals were sampled every 0.4 ns, over a total time interval of 212 ns (532 data points). The time base of the oscilloscope was started by a trigger indicating the passage of a beam particle. Our readout scheme optimized the CPU utilization and the data taking efficiency thanks to the bunch structure of the SPS cycle, where beam particles were provided to our experiment during a spill of 9.6 s, with a repetition period of 48 s. During the spill, all events were sequentially recorded in the internal memory of the scope. We were able to reach, in spill, a data acquisition rate of $\sim 2 \text{ kHz}$, limited by the size of the internal scope buffer. No zero suppression was implemented, so that the event size was constant: $\sim 1.5 \text{ MB}$, largely dominated by the oscilloscope data.

2.3. Experimental data and analysis methods

The purpose of these tests was to split the crystal signals into their scintillation and Cherenkov components in the most

efficient way. We exploited the following differences between these components to achieve this:

- (1) Differences in *directionality*: Contrary to scintillation light, which is emitted isotropically, Cherenkov light is emitted at a characteristic angle by the relativistic (shower) particles that traverse the detector. We measured the signals for different orientations (i.e., angles θ) of the crystal with respect to the beam.
- (2) Differences in *time structure*: Cherenkov light is prompt, while the scintillation mechanism is characterized by one or several time constants, which determine the pulse shape. Detailed measurements of the time structure were performed (at different angles θ) to study the properties of the prompt component in the crystal signals.
- (3) Differences in the *spectral properties*: Cherenkov light exhibits a λ^{-2} spectrum, while the scintillation spectrum is characteristic for the crystal in question. Of course, the extent to which these differences may be observed in the measured signals depends also on the filters and on the wavelength dependence of the quantum efficiency of the light detectors.

The measurements were performed with 50 GeV e^- beams. The angle θ between the crystal axis and the plane perpendicular to the beam line was varied between -55° and 55° , in steps of 5° . At each angle, 50 000 events were collected. In addition, 10 000 randomly triggered events provided pedestal information. For each event, the full time structure of the signals from the two PMTs that read the two sides of the crystal was recorded, as well as the ADC and TDC data from the auxiliary detectors (fiber calorimeter, wire chambers, trigger counters, muon counters).

It is well known that the (scintillation) light yield of PbWO_4 crystals is strongly temperature dependent. In a previous study, we measured this effect to be $-2.6\%/^\circ\text{C}$ [3]. The temperature in the light-tight box housing the crystals was monitored with thermistors. The temperature variations were measured to be small in our setup, typically $< \pm 2^\circ\text{C}$ over a 24-hour cycle. No attempt was made to correct the signals for measured temperature variations. However, during each systematic study of a particular crystal, i.e., over a complete angular scan, or position scan, the temperature did not vary by more than $\pm 1^\circ\text{C}$.

Off-line, the beam chamber information could be used to select events that entered the crystal in a small (typically $10 \times 10 \text{ mm}^2$) region located around its geometric center. The electron beam contained a few percent of muons and hadrons, which could be eliminated with help of the downstream calorimeter and muon counter. Typically, more than half of the events survived these cuts.

2.4. Calibration of the detectors

The PMTs used in these measurements were calibrated with 50 GeV electron beams. The calibrations were carried out at $\theta = 0$, i.e., with the crystal oriented perpendicular to the beam line and the beam hitting the center of the crystal. In this geometry, 50 GeV electrons deposited, on average, 355 MeV in the PbWO_4 crystals, as determined with GEANT-4 Monte Carlo calculations. The absolute calibration of the signals generated by the crystal was only important for the light yield measurements (Section 3.5), which were carried out at $\theta = 30^\circ$. At this angle, the 50 GeV electrons deposited, on average, 578 MeV in the crystals.

For the time structure measurements, no separate calibration effort was performed. We only made sure that the vertical oscilloscope scale was chosen such that no pulse clipping occurred. As the crystals were rotated to larger angles θ , the

⁴ We measured the signal speed to be 0.78c in these cables.

⁵ http://www.tek.com/site/ps/0,,55-13766-SPECS_EN,00.html

signals increased and the scale had to be adjusted, e.g., from 100 to 200 mV to 500 mV full range.

3. Experimental results

The molybdenum doping of the PbWO_4 crystals was intended to achieve two goals:

- a redshift of the scintillation spectrum, and
- an increase in the decay time of the scintillation signals.

The first effect is illustrated in Fig. 3a, which shows the (normalized) emission spectra of PbWO_4 crystals doped with different fractions of molybdenum. The largest effects were observed when a small (0.1%) amount of Mo was added to the undoped crystal, and when this fraction was doubled. Beyond that, the differences were rather small [8].

It turned out that the molybdenum also had undesirable side effects. In particular, it made the PbWO_4 crystal less transparent at short wavelengths. This is illustrated in Fig. 3b, which shows that the UV absorption edge clearly depended on the doping fraction [9]. As described in the following subsections, this effect had important consequences for the detection of the Cherenkov light, especially since the available filters for selecting this light were opaque beyond a wavelength that was close to this

absorption edge. The cutoff wavelengths of the three UV transmission filters (see Fig. 1) are also indicated in Fig. 3. The strength, the purity and the attenuation characteristics of the Cherenkov signals thus depended on the characteristics of the narrow bandwidth domain between the absorption edge and the emission spectrum selected by the transmission filter.

In the following, we concentrate first predominantly on the effects of the filter choice, and later on the effects of the doping concentration.

3.1. Time structure of the signals

The filters mounted on the two ends of the crystal were intended to transmit predominantly Cherenkov light on one end and scintillation light on the other end. One way to see how well this worked is to look at the time structure of the signals. Fig. 4 shows the average time structure of the signals from 50 GeV electrons traversing a PbWO_4 crystal doped with 0.3% Mo, for three different filters used to select Cherenkov light (Fig. 4a), and for one filter intended for the scintillation light (Fig. 4b). The crystal was in all cases oriented at $\theta = 30^\circ$, such as to maximize the detection efficiency for Cherenkov light. Since the scale of the oscilloscope and the gain of the PMT were the same for all three Cherenkov measurements, we can interpret these results not only in terms of differences in the time structure, but also according to the amplitude of the signals. The fact that the transmission curve of the UG11 filter was located very close to the UV absorption edge of the crystal is illustrated by the observation that an increase of the effective bandwidth for detecting Cherenkov light by ~ 10 nm led to a very substantial increase in the average Cherenkov signals: the signals measured with the U330 filter were on average a factor 5–10 larger than those measured with the UG11 filter. The effect of increasing the bandwidth further, by using the UG5 filter, was clearly much smaller.

The very narrow effective bandwidth for detecting Cherenkov light with a UG11 filter was earlier observed from measurements of crystals doped with 1% and 5% Mo, respectively [5]. The small reduction in the bandwidth resulting from a 5 nm shift in the UV absorption edge (see Fig. 3b) reduced the Cherenkov signal by about a factor of three in those measurements.

Fig. 4 also shows that the time structures for all three filters used on the Cherenkov side of the crystal were very different from the time structure measured for the average scintillation signal. Even with UG5, the contamination from scintillation light, which should appear as a tail resembling that of Fig. 4b superimposed on an otherwise prompt signal, was very small. This confirms the results from the radioluminescence measurements [10], which showed that the molybdenum impurity shifts a large fraction of the scintillation light to the wavelength region beyond 500 nm. The extent to which scintillation light would contaminate the Cherenkov signals for the different filters and doping concentrations may be estimated from Fig. 3.

3.2. The Cherenkov/scintillation signal ratio

Another way to examine the purity of the Cherenkov signals, and the effects of changing the filter and/or the Mo content of the crystal on that purity, is by studying the angular dependence of the ratio of the signals measured on both ends of the crystal. The larger the contamination of scintillation light in the Cherenkov signals, the smaller the angular dependence of that signal ratio.

Fig. 5a shows the Cherenkov/scintillator signal ratio (hereafter called the R/L ratio) as a function of the angle of incidence θ of the incoming beam particles for a crystal with a Mo concentration of 0.3%, where the Cherenkov signal was selected by means of a U330 filter. The angular dependence of this ratio exhibits indeed

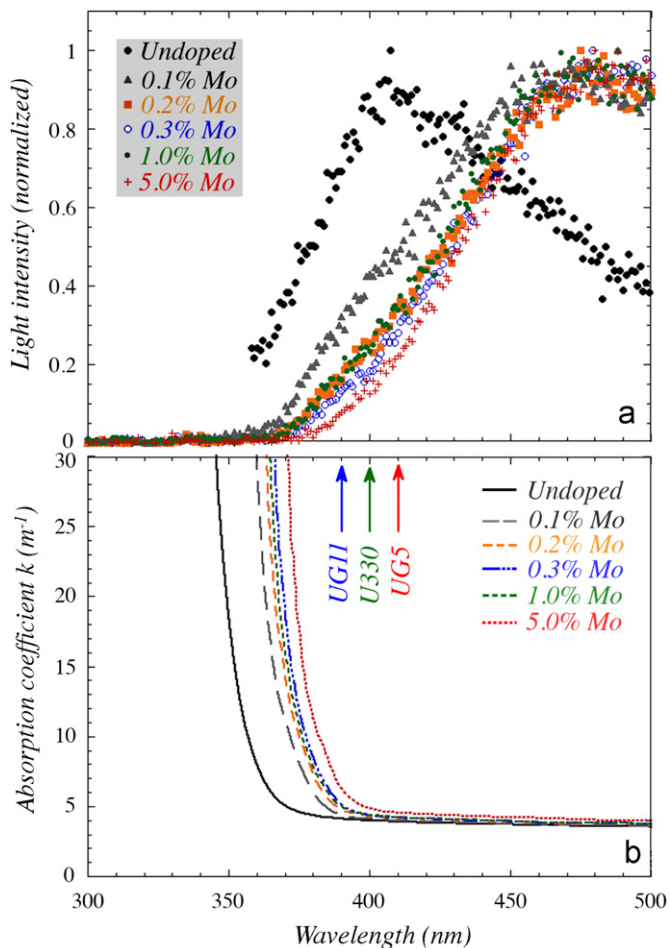


Fig. 3. Normalized emission spectra for PbWO_4 crystals doped with different fractions of molybdenum, measured with radioluminescence (a). The absorption coefficient as a function of wavelength, for PbWO_4 crystals doped with different fractions of molybdenum (b). The cutoff wavelengths of the three UV transmission filters are also indicated.

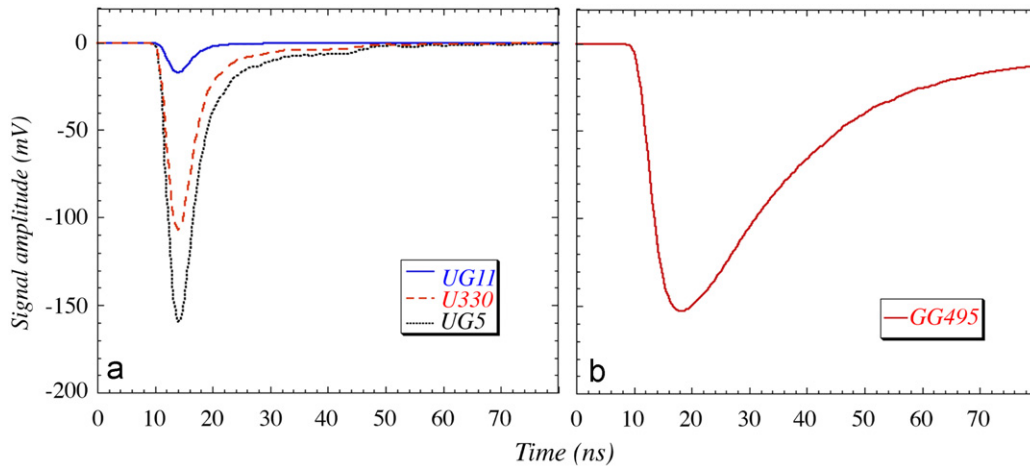


Fig. 4. Average time structure of the signals from 50 GeV electrons traversing a PbWO_4 crystal doped with 0.3% Mo. Results are given for different filters. The crystal was oriented at an angle $\theta = 30^\circ$, such as to maximize the detection efficiency of Cherenkov light. Results are given for several filters intended to detect the Cherenkov signal (a) or the scintillation signal (b).

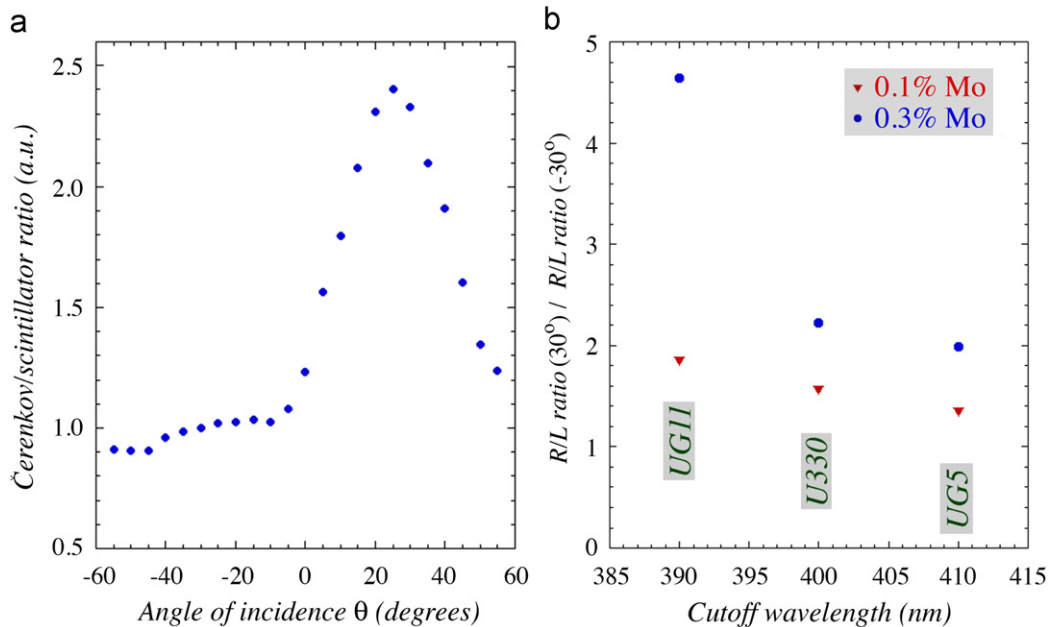


Fig. 5. The R/L signal ratio as a function of the angle of incidence of the beam particles, for a Mo concentration of 0.3% and a U330 filter mounted on the Cherenkov (R) end of the PbWO_4 crystal (a). The ratio of the R/L signal ratios measured at $\theta = 30^\circ$ and -30° , for different filters used to enhance the relative Cherenkov contribution to the R signal, and two different Mo concentrations (b).

the characteristics expected for an R signal dominated by Cherenkov light. The ratio peaks near the angle at which Cherenkov light is most efficiently detected ($\theta = 90^\circ - \theta_c = 27^\circ$). The R/L ratio at $\theta = 30^\circ$ was measured to be about 2.4 times larger than at $\theta = -30^\circ$. We used the ratio of the R/L ratios measured at $\theta = 30^\circ$ and -30° as a figure of merit indicating the purity of the Cherenkov (R) signal. This figure of merit is shown for the three different Cherenkov filters in Fig. 5b.

Comparable data for these three different filters were only taken for the PbWO_4 crystal doped with 0.1% Mo. It is interesting to note that the plotted ratio is significantly larger for the measurements performed on the 0.3% Mo crystal. This is consistent with the observation (Fig. 3) that the fraction of transmitted scintillation light by any of the three UV filters was larger for the 0.1% crystal than for the 0.3% one. This difference apparently outweighed the increase in the Cherenkov signal resulting from the 10 nm shift in the UV absorption edge.

Especially for the measurement with the UG11 filter, the difference amounts to more than a factor of two. In the following subsection, we demonstrate that differences in the light attenuation characteristics may also have contributed to the size of that effect.

3.3. Effects of light attenuation

One of the most undesirable consequences of a small effective bandwidth for the Cherenkov signal is the strong attenuation of the detected light. The strongly increasing self-absorption near the UV absorption edge is responsible for this phenomenon, which we noticed earlier from measurements on PbWO_4 crystals doped with 1% and 5% Mo and equipped with a UG11 filter to detect the Cherenkov light [5]. The position dependence of the response makes such crystals impractical as particle detectors.

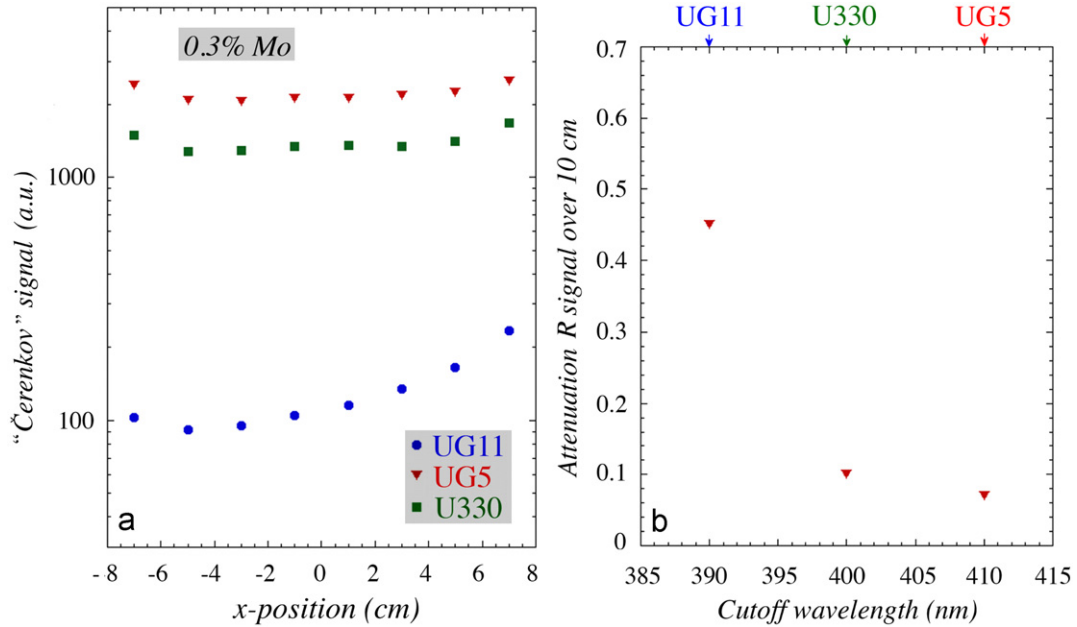


Fig. 6. The position dependence of the R signal, for different filters used to enhance the relative contribution of Čerenkov light to the R signal, for a Mo concentration of 0.3% (a). The relative change in the R signal over a distance of 10 cm, for different filters used to enhance the relative Čerenkov contribution to the R signal (b).

The increased bandwidth offered by the other Čerenkov filters greatly alleviated this problem, as illustrated in Fig. 6. Fig. 6a shows the results of a position scan, in which the 50 GeV electron beam was moved in steps of 2 cm along the longitudinal axis of the crystal, doped with 0.3% Mo in this case. Whereas the crystal response dropped by about a factor of two over 10 cm in the case of the UG11 filter, the decrease was < 10% when a U330 or UG5 filter was used to detect the Čerenkov light (Fig. 6b).

We conclude that UG11 not only transmitted about an order of magnitude less light than the U330 and UG5 filters, but also that the little light it did transmit also had wavelengths close to the UV absorption edge of the PbWO₄ crystal. As a result, it was much more strongly attenuated than the light transmitted by the other two filters. At $\theta = 30^\circ$, the path length of the Čerenkov light detected by PMT R is, on average, shorter than that of the isotropically emitted scintillation light. As a result, the Čerenkov component is less affected by the strong light attenuation than the scintillation component. This translates into a larger Č/S signal ratio than for crystal/filter combinations in which light attenuation plays a less important role (see Fig. 5).

3.4. Changing the doping concentration

After having concentrated in the previous subsections on the effects of the filters, we now examine in some detail the effects of the concentration of the molybdenum impurity on the performance of the PbWO₄ crystals. Whereas the effects of changing the transmission spectrum of the filter intended to detect the Čerenkov light produced by the showering particles were more or less straightforward to understand, some of the effects observed as a result of changes in the Mo doping fraction were less obvious.

We performed systematic measurements for five different concentrations using the U330 filter for generating the Čerenkov signals, since this filter yielded both a good amplitude and adequate purity of the Čerenkov signals. Fig. 7 shows the average time structure of the signals produced by the light traversing this filter. The signals measured for crystals doped with 0.2%, 0.3% and 1% Mo were almost carbon copies of each other. The signals

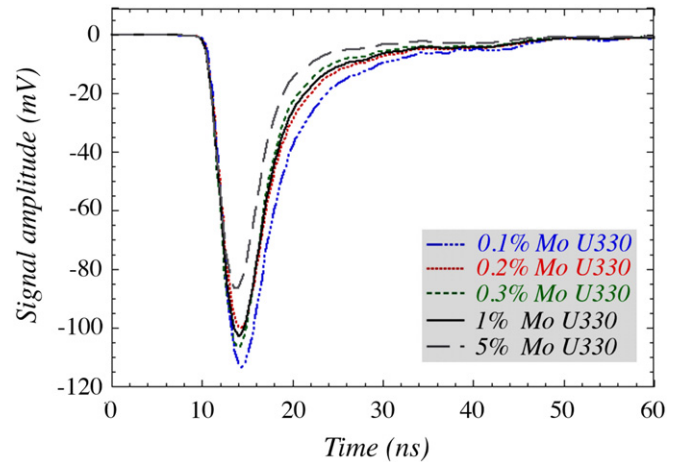


Fig. 7. Average time structure of the signals from the light traversing a U330 filter, for PbWO₄ crystals with different levels of Mo doping.

measured for the 0.1% crystal had a slightly larger amplitude and also seemed to contain a somewhat larger contaminating scintillation component. The opposite effect was observed for the crystal with the largest doping fraction (5%), whose signals had a smaller amplitude and seemed to be more purely of Čerenkov origin than the others.

These effects are, at least qualitatively, in agreement with expectations on the basis of Fig. 3. As the Mo fraction increases, the total amount of Čerenkov light decreases, as a result of the gradually shifting UV absorption edge. Going from 0.1% to 5%, this edge shifts by ~ 15 nm, and reduces the effective bandwidth by about one third. In addition, the fraction of the scintillation light transmitted by the filter decreases even more from 5.8% to 1.5%.

Based on the reduced effective bandwidth, one would also expect to see, for a given filter, increased purity of the Čerenkov signals and shorter attenuation lengths, as the molybdenum fraction increases. Fig. 8 shows how the purity of the Čerenkov signals, derived from the angular dependence of the Čerenkov/scintillation signal ratio (a), and the attenuation of the

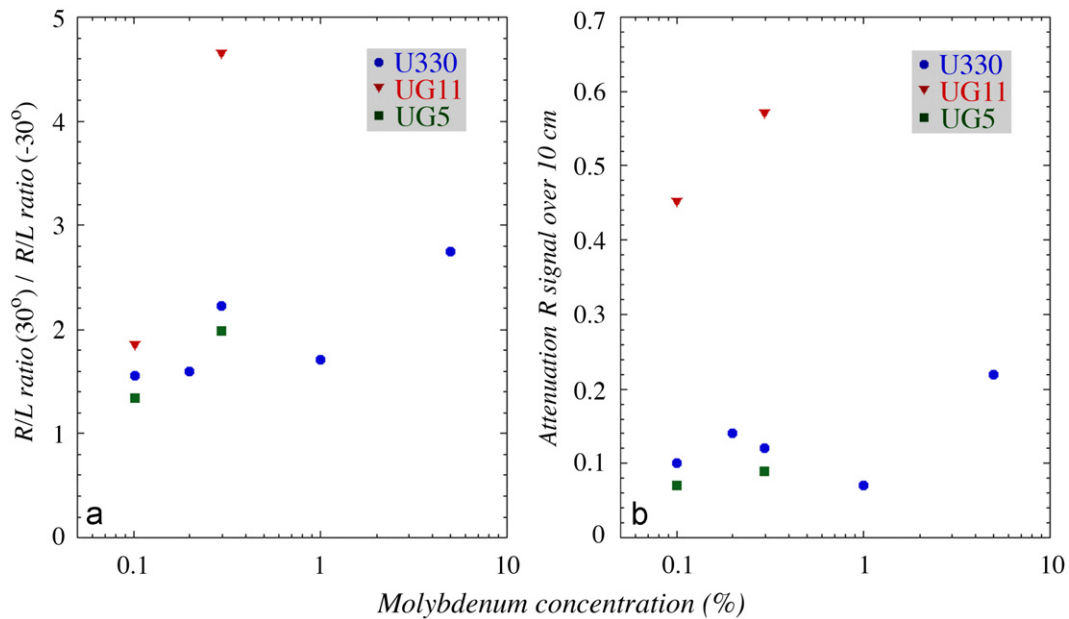


Fig. 8. The ratio of the R/L signal ratios measured at $\theta = 30^\circ$ and -30° (a), and the relative change in the R signal over a distance of 10 cm (b), as a function of the molybdenum concentration in the PbWO_4 crystal.

Cherenkov light (b) depended on the concentration of molybdenum in the PbWO_4 crystals. Results are given for all crystal/filter combinations used in this study.

With the exception of results obtained for the 1% Mo crystal, the experimental data seem to confirm the expected trend. With the U330 filter, the purity parameter $R/L(30^\circ)/R/L(-30^\circ)$ increased from 1.6 (0.1% Mo) to 2.8 (5% Mo), and the signal reduction over 10 cm changed from 10% (0.1% Mo) to 22% (5% Mo). Even though the results obtained with other filters were much more scarce, they did confirm the observed trend that the purity and the effects of light attenuation increase with the molybdenum concentration.

It should be emphasized that each of these crystals was the result of a completely separate production process. Even though the Mo concentration was the only parameter that was deliberately varied, other factors may have deviated as well. Also, the crystals with the highest Mo concentration (1%, 5%) were produced one year before the crystals with the lower concentrations. We already noted earlier (Fig. 3a) that the redshift of the emission spectrum in the 1% crystal was about the same as for the 0.2% crystal. This means that the relative contamination of scintillation light in the U330 signals was similar for both crystals. Therefore, it is not a complete surprise that the results on Cherenkov signal purity and light attenuation are somewhat anomalous for the 1% Mo crystal.

The fact that details of the production process other than the fraction of molybdenum incorporated in the melt may have affected the properties of the crystals studied here, is also corroborated by the observation that some of these properties were quite different for crystals with nominally the same composition, but produced with another crystal growing method (Bridgman versus Czochralski).

3.5. Effects of the signal integration time

In the previous subsections, we have shown how the signal composition varies as a function of the molybdenum doping concentration, and of the filter that is used to select the Cherenkov light. However, there is a third variable that may be used to that effect, namely the time interval over which the signals are integrated. Because of the different time structures of the two

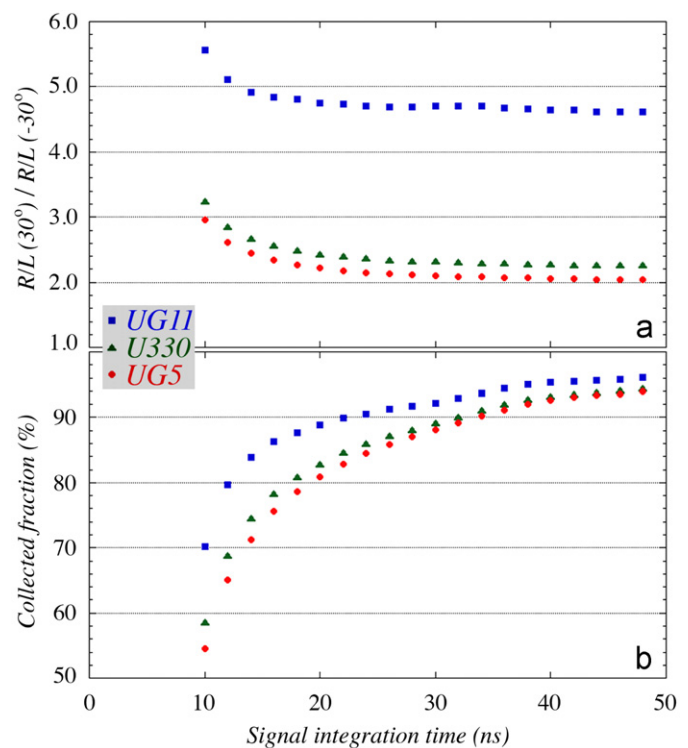


Fig. 9. The Cherenkov/scintillator ratio (a) and the fraction of the UV-filtered light collected (b) as a function of the signal integration time. Results for the 0.3% Mo doped PbWO_4 crystal and three different filters used to select the Cherenkov component of the signals.

signal components, one may use the signal integration time, for example, to further purify the Cherenkov signals, of course at the cost of losing some precious photoelectrons.

This is illustrated in Fig. 9, which shows the Cherenkov/scintillator ratio and the fraction of the UV-filtered light collected as a function of the signal integration time, for the 0.3% Mo doped PbWO_4 crystal and the three different filters used to select the

Cherenkov component of the signals. In order to significantly improve the purity of the Cherenkov signals, signal integration times shorter than 20 ns have to be used, during which time interval 80–90% of the UV light is collected, depending on the filter. These results confirm our earlier observation that the UG11 signals contain the smallest contamination of scintillation light. They also show that similar levels of purity can be obtained with the other filters, by reducing the signal integration time.

We studied the effects of the integration time also for crystals with other levels of molybdenum doping. Fig. 10 shows the Cherenkov/scintillator ratio and the fraction of the UV-filtered light collected as a function of the signal integration time, for five different crystals with a doping level varying from 0.1% to 5.0%. The Cherenkov signal was obtained by means of a U330 filter for these measurements. These measurements confirm that the purity of the Cherenkov signals increases with the Mo-concentration, disregarding the odd behavior of the 1.0% crystal. For a given integration time, the fraction of the total collected charge, as well as the ratio of the R/L signal ratios measured at $\theta = 30^\circ$ and -30° increases with the Mo-concentration. As before, it requires signal integration times shorter than 20 ns to affect this purity significantly.

3.6. The Cherenkov light yield

One of the main reasons why we started studying high- Z crystals as candidate dual-readout calorimeters was the very low Cherenkov light yield obtained in the fiber calorimeter with which the dual-readout ideas were pioneered: 8–18 photoelectrons per GeV deposited energy, depending on the type of fibers [6]. Unfortunately, the use of a UG11 UV filter reduced the Cherenkov light yield of our first batch of $\text{PbWO}_4:\text{Mo}$ crystals to similar

values [5]. However, the increased bandwidth offered by the U330 and UG5 filters turned out to be also beneficial in this respect.

The method with which we determined the Cherenkov light yield was based on the assumption that, for a given amount of energy deposited in the crystal, the fluctuations in the numbers of scintillation photons were negligibly small compared to those in the numbers of Cherenkov photons. If this assumption were not entirely valid, then the Cherenkov light yields listed below would represent in fact a *lower limit*.

Fig. 11 serves to illustrate the method. First, we integrated each scintillation signal over the entire time structure. This integrated charge was used as a measure for the energy deposited by the beam particle (a 50 GeV electron) in the crystal. We used the data obtained at $\theta = 30^\circ$ for this analysis. At this angle, the fraction of *detected* Cherenkov photons reached a maximum and the electrons traversed slightly more than two radiation lengths in the crystal. Monte Carlo simulations showed that they deposited on average 0.578 GeV in this process. This result served as the basis for the calibration, and made it possible to relate the integrated scintillator signals to the amount of energy deposited in the crystal. Fig. 11a thus shows the event-by-event distribution of the energy lost by the showering electrons.

This distribution was subdivided into 20 bins. For each bin, the signal distribution on the *opposite side* of the crystal, i.e., the Cherenkov side, was measured. The fractional width of this distribution, $\sigma_{\text{rms}}/C_{\text{mean}}$, is plotted in Fig. 11b versus the average scintillator signal in this bin, or rather versus the inverse square root of this signal ($S^{-1/2}$). It turned out that this fractional width scaled perfectly with this variable, i.e., with $E^{-1/2}$. Since the relationship between the energy E and the scintillation signal S is given by the calibration described above, it is also possible to indicate the energy scale in Fig. 11b. This is done on the top horizontal axis.

The fact that $\sigma_{\text{rms}}/C_{\text{mean}}$ scales with $E^{-1/2}$ means that the energy resolution is completely determined by stochastic processes which obey Poisson statistics. In this case, fluctuations in the Cherenkov light yield were the only stochastic processes that played a role, and therefore the average light yield could be directly determined from this result: 55 photoelectrons per GeV deposited energy. For an energy deposit of 1 GeV, this led to a fractional width of 13.5%.

The results shown in Fig. 11 concern the crystal doped with 0.3% Mo. The same analysis has been repeated for all crystal/filter combinations. The Cherenkov light yield results for all combinations are summarized in Table 1. As before, the most complete set of experimental results was obtained with the U330 filter. The Cherenkov light yield was found to be about an order of magnitude larger than with the UG11 filter. This was a direct consequence of the strongly increased transmission in the wavelength range around 400 nm, where the PMTs reached their maximum sensitivity. The UG5 result shows that a further increase of the bandwidth on the right hand side did relatively little for the Cherenkov light yield. The light yield measured with the U330 filter also seemed to be relatively insensitive to the molybdenum fraction. Only at the highest Mo-concentration (5%) did we start to see the effect of the shifting UV absorption edge (Fig. 3b).

We should re-emphasize that the results listed in Table 1 are, strictly speaking, lower limits. This is because they are based on the assumption that the energy deposited in each of the 20 different bins was constant. Fluctuations in the scintillation light yield, combined with the chosen bin widths, increase the fractional widths of the Cherenkov signal distributions shown in Fig. 11b. This effect might also limit the increase seen with the UG5 filter, where a significant fraction of scintillation light was mixed in with the Cherenkov signals.

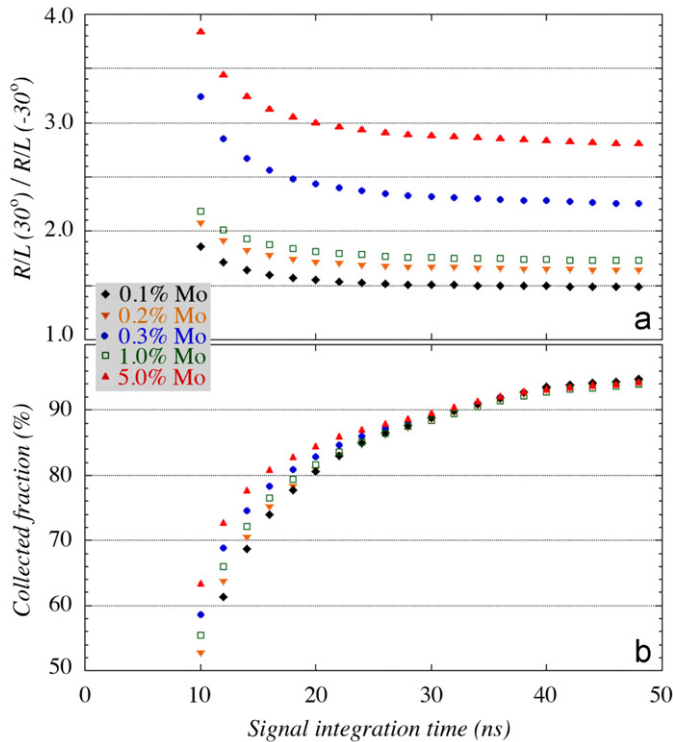


Fig. 10. The Cherenkov/scintillator ratio (a) and the fraction of the UV-filtered light collected (b) as a function of the signal integration time, obtained with a U330 filter for selecting the Cherenkov signal component. Results for PbWO_4 crystals with five different molybdenum doping levels.

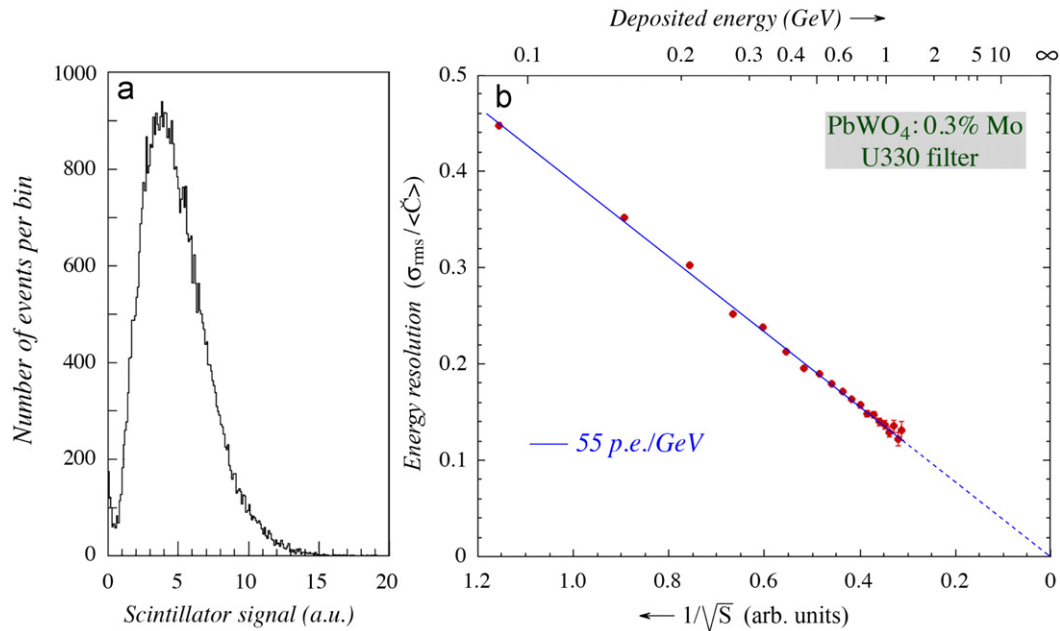


Fig. 11. The scintillator signal distribution for 50 GeV electrons traversing the crystal at $\theta = 30^\circ$ (a) and the fractional width of the Cherenkov signal distribution as a function of the amount of energy deposited in the crystal, as derived from the scintillator signal (b). The PbWO_4 crystal was doped with 0.3% Mo. See the text for more details.

Table 1

Cherenkov light yield measured for PbWO_4 crystals doped with different fractions of molybdenum.

Mo fraction (%)	UG11	U330	UG5
0.1	4.6	62.1	
0.2		56.7	
0.3	5.9	55.3	64.9
1.0		58.3	
5.0		38.3	

The results are given in photoelectrons per GeV, and measured with 50 GeV electrons traversing the crystal at an angle $\theta = 30^\circ$, i.e., close to the Cherenkov angle.

4. Conclusions

We have investigated the properties of PbWO_4 crystals doped with small amounts of molybdenum. This study was carried out to examine if and to what extent such added impurities would improve the suitability of PbWO_4 crystals for the purpose of dual-readout calorimetry, and how sensitive the improvement would be to the molybdenum fraction. Earlier studies had revealed that the self-absorption of Cherenkov light and the related reduction in Cherenkov light yield of the Mo-doped crystals were unacceptably large.

It turned out that both factors could be strongly alleviated, not so much by changing the doping level, but primarily by using a less restrictive filter for generating the Cherenkov signals. The cause of the problems encountered in our initial studies was the very narrow bandwidth for which Cherenkov light was accepted, between the UV absorption edge of the crystal and the transmission edge of the filter. Lowering the Mo level lowers the former, while changing the filter may shift the latter to longer wavelengths. By using a U330 or UG5 filter instead of the UG11 filter used in our initial studies, the Cherenkov light yield was increased by an order of magnitude, while the attenuation of this light was reduced to $< 10\%$ over the length of the crystal. This increased

acceptance decreased the purity of the Cherenkov signal somewhat, but because of the difference between the prompt nature of that component, any contamination from a signal with a decay time of 26 ns could be easily recognized and eliminated on the basis of the time structure of the overall crystal signal.

While the highest concentration level of molybdenum used in these studies (5%) led to some noticeable disadvantageous effects, all concentrations between 0.1% and 1% produced largely similar results for what concerns signal purity, light yield and light attenuation of the Cherenkov component.

However, a final word of caution is warranted here. All studies on which we have reported here were performed using only *one* crystal of each specified composition. As illustrated by the results in Section 3.4, factors other than the molybdenum content might have affected the results. For this reason, it is not possible on the basis of the data presented here to choose a particular Mo concentration as producing superior results. Any PbWO_4 crystal with a molybdenum concentration in the range from 0.1% to 1.0% seems to be adequate for dual-readout calorimetry applications.

Acknowledgements

We thank CERN for making particle beams of excellent quality available. We are also indebted to the *Radiation Instruments & New Components* company in Minsk (Belarus), which produced the crystals tested in this study in a timely manner and according to our specifications. Drs. M. Nikl and A. Vedda, together with their collaborators, were kind enough to perform the measurements of the emission and absorption spectra of the crystals, respectively, and we thank them for their interest and generosity. This study was carried out with financial support of the United States Department of Energy, under Contract DE-FG02-07ER41495, and by Italy's Istituto Nazionale di Fisica Nucleare.

References

- [1] R. Wigmans, N. J. Phys. 10 (2008) 025003.
- [2] N. Akchurin, et al., Nucl. Instr. and Meth. A 582 (2007) 474.

- [3] N. Akchurin, et al., Nucl. Instr. and Meth. A 593 (2008) 530.
- [4] N. Akchurin, et al., Nucl. Instr. and Meth. A 595 (2008) 359.
- [5] N. Akchurin, et al., Nucl. Instr. and Meth. A 604 (2009) 512.
- [6] N. Akchurin, et al., Nucl. Instr. and Meth. A 536 (2005) 29.
- [7] N. Akchurin, et al., Nucl. Instr. and Meth. A 537 (2005) 537.
- [8] The radioluminescence measurements of the emission spectra of the crystals were performed by M. Nikl at the Institute of Physics AS CR in Prague (Czech Republic) with a custom-made 5000M Horiba Yobin Yvon spectrofluorometer, equipped with a steady-state X-ray tube (40 kV, tungsten cathode). The emission spectra were corrected for the spectral response of the detection part of the system.
- [9] The measurements of the wavelength dependent absorption characteristics of the crystals were performed at the Department of Material Science at the University of Milano-Bicocca, by A. Vedda, with a Perkin Elmer Lambda 950 spectrophotometer. The measurements were performed at room temperature, along the crystal length, and were not corrected for effects of reflectivity.
- [10] M. Nikl, et al., J. Appl. Phys. 91 (2002) 2791.